AIP | Applied Physics Letters

Abnormal electronic transition variations of lanthanum-modified lead zironate stannate titanate ceramics near morphotropic phase boundary: A spectroscopic evidence

X. Chen, K. Jiang, Z. G. Hu, X. F. Chen, G. S. Wang et al.

Citation: Appl. Phys. Lett. **101**, 011914 (2012); doi: 10.1063/1.4733683
View online: http://dx.doi.org/10.1063/1.4733683
View Table of Contents: http://apl.aip.org/resource/1/APPLAB/v101/i1
Published by the American Institute of Physics.

Abnormal electronic transition variations of lanthanum-modified lead zironate stannate titanate ceramics near morphotropic phase boundary: A spectroscopic evidence

X. Chen (陈啸),[1] K. Jiang (姜凯),[1] Z. G. Hu (胡志高),[1,a)] X. F. Chen (陈学锋),[2] G. S. Wang (王根水),[2] X. L. Dong (董显林),[2] and J. H. Chu (褚君浩)[1]
[1]*Key Laboratory of Polar Materials and Devices, Ministry of Education, Department of Electronic Engineering, East China Normal University, Shanghai 200241, China*
[2]*Shanghai Institute of Ceramics, Chinese Academy of Sciences, Shanghai 200050, China*

(Received 28 May 2012; accepted 20 June 2012; published online 6 July 2012)

The structure-related optical response of $(Pb_{1-1.5x}La_x)(Zr_{0.42}Sn_{0.40}Ti_{0.18})O_3$ (100*x*/42/40/18) ceramics with different compositions has been investigated. Based on x-ray diffraction, the phase transition from rhombohedral to tetragonal structure is revealed between compositions of $x = 2.6\%$ and 2.8% near morphotropic phase boundary (MPB). Correspondingly, abnormal spectral response in the photon energy from 1.4 to 6.1 eV is observed near MPB. Furthermore, the blue shift of the two critical points related parameters, which is obtained from fitting the reflectance spectra, indicates that the variation of electronic band structure near MPB is responsible for the anomalous behavior. © *2012 American Institute of Physics*. [http://dx.doi.org/10.1063/1.4733683]

In the past few decades, the complex Pb-based ABO_3 perovskite materials have attracted much attentions, due to the excellent properties (ferroelectric, antiferroelectric, piezoelectric, and pyroelectric) obtained in the compositions close to morphotropic phase boundary (MPB).[1–4] $Pb(ZrSnTi)O_3$ (PZST) pseudoternary system is a typical one. Compared to the parent compound, $Pb(Zr_{1-y}Ti_y)O_3$ (PZT), incorporation of Sn^{4+} in the *B*-cation makes PZST much easier in compositional tailoring rather than the narrow region centered at $y = 0.50$ in PZT.[5] The phase diagram of PZST was established by Berlincourt.[6] In the compositions near the boundary between ferroelectric-rhombohedral phase and antiferroelectric-tetragonal phase, a switching from one phase to another could be utilized by applying enough electrical or temperature field.[7,8] Accompanied by the phase transition, the compounds possess unique properties, such as double hysteresis, large strain, considerable pyroelectric coefficient and huge electrocaloric effect, which makes them as potential materials in applications of high-energy-storage capacitors, high-strain transducers or actuators, infrared detectors, and cooling devices.[1]

Lanthanum (La) modification in the *A*-cation was often utilized to obtain better physical properties, such as enhancement of the antiferroelectric (AFE) phase and inducement of a diffused phase transition.[5] In addition, La-modification also has a significant influence on microstructure.[9] Nevertheless, the relationship between the microstructure and macroscopic properties is far from the clarification. Chan *et al.*[10] reported the electrical properties of La-modified lead zironate stannate titanate (PLZST) with different microstructure, which was induced by La-introduction. It was observed that pure PZST was ferroelectric (FE) state at room temperature. However, La concentration of 2 mol. % destabilizes FE state and transforms into an incommensurate AFE state. Further increasing of La composition enhanced the stability of the AFE state at room temperature. Due to the complexity of physical phenomena across the MPB, more investigations on the structure-related macroscopic properties are necessary. As the important macroscopic properties, optical properties are strongly related to the electronic structures, which can be essentially determined by the crystal structures. By modeling the experimental spectra, optical function and the accurate positions of critical points (CPs) on the electronic structure can be extracted.[11] Therefore, one can investigate the phase transition behavior by analyzing electronic band structures and/or dielectric functions owing to the lattice variation. Compared to the electrical study, spectral technique takes advantage of nondestructive measurement and avoiding interface effects from electrodes, etc. On the other hand, it can provide an important insight on the performance of perovskite oxide-based optoelectronic devices.

In this letter, La-modification inducing phase transition of PLZST ceramic was observed with the aid of x-ray diffraction (XRD) and spectral reflectance techniques. Correspondingly, the abnormal changes of optical properties and electronic band structure during the phase transition are discussed in detail.

Because the compound $Pb(Zr_{0.42}Sn_{0.40}Ti_{0.18})O_3$ locates near the MPB,[7] the compositions investigated are $(Pb_{1-1.5x}La_x)(Zr_{0.42}Sn_{0.40}Ti_{0.18})O_3$ (100*x*/42/40/18), where $x = 1\%$, 2%, 2.6%, 2.8%, 3.4%, and 3.6% (hereafter denoted as L1, L2, L2.6, L2.8, L3.4, and L3.6, respectively). The bulk ceramics were fabricated by solid state reactions, using the appropriate amount of reagent grade raw materials of lead tetraoxide (Pb_3O_4), zirconium dioxide (ZrO_2), titanium dioxide(TiO_2), tin oxide (SnO_2), and lanthanum oxide (La_2O_3). The sintering process was carried out in a lead rich environment in order to minimize lead volatilization. The samples were sintered at 1300 °C for 1 h in air atmosphere. Then all samples with the diameter of 13 mm and the thickness of 1 mm were single-side polished for the spectral measurements. The crystalline

a)Author to whom correspondence should be addressed. Electronic mail: zghu@ee.ecnu.edu.cn. Tel.: +86-21-54345150. Fax: +86-21-54345119.

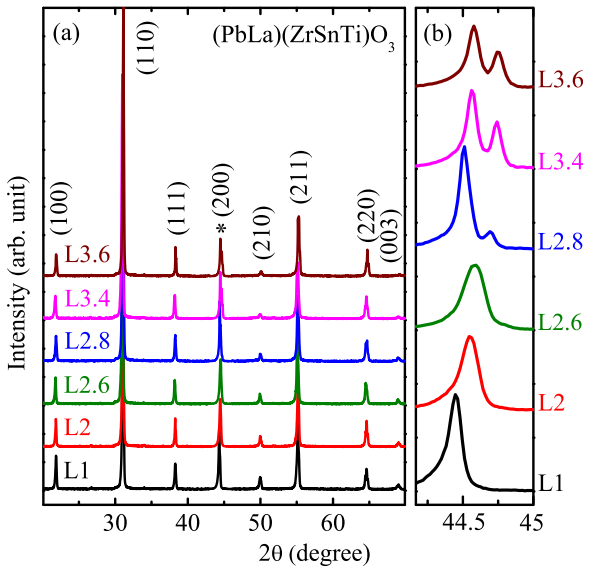

FIG. 1. (a) X-ray diffraction patterns of the PLZST ceramics with different La composition. The label (*) indicates the (200) peak in the rhombohedral phase, which splits to (002) and (200) peaks in the tetragonal phase. (b) The enlarged region for the diffraction peaks at $2\theta \approx 45°$.

structures of the PLZST ceramic were investigated by XRD using a Ni filtered Cu-Kα radiation operated at 40 kV and 200 mA (D/MAX-2550V, Rigaku Co.). The near-normal incident (about 8°) reflectance spectra were recorded by a double beam ultraviolet-infrared spectrophotometer (PerkinElmer Lambda 950) at the photon energy region from 1.4 to 6.1 eV (200-880 nm) with a spectral resolution of 1 nm, using an aluminum mirror as reference. Note that all of the measurements were carried out at room temperature (RT).

Fig. 1(a) shows the XRD patterns of the PLZST ceramics. The strongest (110) diffraction peak is located at about 31° and other weaker peaks (100), (111), (200), (210), (211), (220), and (003) also appear. It indicates that the samples are pure perovskite structure and there is no secondary pyrochlore structure. The patterns show high similarity to those of single crystal powder,[12] suggesting good qualities of the PLZST ceramics. Because the difference between a and c inheres in tetragonal lattice system, it is well known that the peak splits at $2\theta \approx 45°$ when the transition from the rhombohedral phase to tetragonal phase occurs. The phenomena could be clearly observed in the enlarged patterns of Fig. 1(b). For the samples L1, L2, and L2.6, the peaks are single, whereas the sample L2.8 shows a split into a high peak and a small hump, whose intensity increases with increasing La composition. The splitting trend could be uniquely attributed to the phase transition from the single (200) diffraction peak of rhombohedral structure to (200) and (002) peaks of tetragonal one. Note that the phase transition is found to appear at about the La composition of 2.6%. As can be seen in Fig. 1(b), the shift of peaks towards to a higher diffraction angle is resulted from the fact that the ironic radius of La^{3+} (1.36 Å) is smaller than that of Pb^{2+} (1.49 Å). The lattice parameters were listed in Table I, which are slightly smaller than that of single crystal reported by Xue *et al.*[13] The value of a decreases generally from 4.083 Å to 4.082 Å in the rhombohedral structure for the La composition of less than 2.6%. The similar reduction could be recognized in the value of c for the rhombohedral structure. This variation could also be attributed to the La introduction with smaller ironic radius. It should be emphasized that the similar phenomena can be observed in (PbLa)(ZrTi)O_3 system.[14] However, the parameter a increases for the ceramics in the tetragonal structure except for sample L3.4, which has the minimal value of 4.076 Å. It should be noted that an evident variation of the lattice parameters could be observed when the phase transition takes place. Thus, one can expect that there will be different spectral response for the PLZST ceramics with the rhombohedral and tetragonal phases, respectively.

In order to extract the optical functions from the reflectance spectra, a dielectric function model should be applied. The optical properties of the PLZST ceramics are analyzed via fitting the reflectance spectra with reasonable dielectric function model. For the PLZST ceramics, double Tauc-Lorentz (DTL) oscillator model is adopted as the following: $\varepsilon_1(E) = \varepsilon_\infty + \frac{2}{\pi} P \int_0^\infty \frac{\xi \varepsilon_2(E)}{\xi^2 - E^2} d\xi$, $\varepsilon_2(E) = \sum_{j=1}^{2} \frac{A_j E_{pj} \Gamma_j (E - E_{tj})^2}{(E^2 - E_{pj}^2)^2 + \Gamma_j^2 E^2} \frac{1}{E}$. Where ε_∞ is the high-frequency dielectric constant, P is the Cauchy principal part of the integral, E is the incident photon energy, A_j, E_{pj}, Γ_j, and E_{tj} is the amplitude, peak position energy, broadening term, and Tauc gap energy of the jth oscillator, respectively. It should be emphasized that the DTL model abides by the Kramers-Krönig transformation in the entirely measured photon energy region.[15] At near-normal incidence, the dielectric functions are related to the reflectance R by the Fresnel formula: $R = |(\sqrt{\varepsilon(E)} - 1)/(\sqrt{\varepsilon(E)} + 1)|^2$. A least-squares-fitting procedure employing

TABLE I. The lattice constants and parameter values of the Double Tauc-Lorentz model for the PLZST ceramics with different La composition obtained by fitting the ultraviolet-near-infrared reflectance spectra in Fig. 2.

	Lattice constants				TL1				TL2			
Samples	a (Å)	c (Å)	α (°)	ϵ_∞	A_1 (eV)	E_{p1} (eV)	Γ_1 (eV)	E_{t1} (eV)	A_2 (eV)	E_{p2} (eV)	Γ_2 (eV)	E_{t2} (eV)
L1	4.083	4.083	89.90	2.96	86.7	3.38	1.43	3.42	114	4.16	2.27	4.48
L2	4.082	4.082	89.90	3.04	89.5	3.38	1.33	3.42	90	4.22	2.81	4.40
L2.6	4.082	4.082	89.90	3.01	170	3.43	1.64	3.40	210	4.36	2.84	4.43
L2.8	4.086	4.075	90.00	3.15	119	3.59	1.60	3.37	194	4.34	2.92	4.38
L3.4	4.076	4.079	90.00	3.05	114	3.57	1.48	3.42	172	4.35	3.44	4.35
L3.6	4.085	4.067	90.00	3.09	101	3.50	1.42	3.42	122	4.31	3.65	4.34

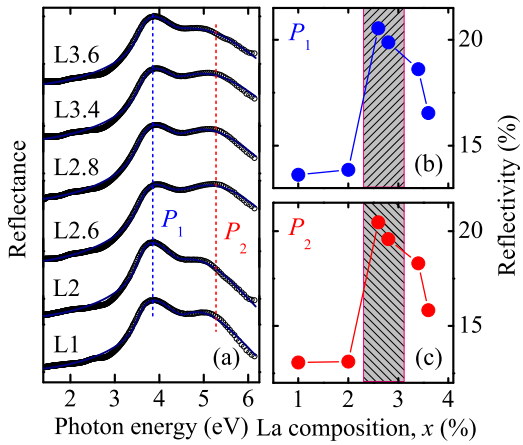

FIG. 2. (a) The experimental (dotted lines) and calculated (solid lines) reflectance spectra of the PLZST ceramics. The spectral data are shifted in the ordinate for clarity. The reflectivity variations of P_1 and P_2 as the La composition increasing are shown in (b) and (c), respectively. Note that the shade parts indicate the phase transition region.

the modified Levenberg-Marquardt algorithm is used. By optimizing the fitting errors between the experimental and calculated data, the best-fit parameter values of the model (i.e., dielectric functions) can be obtained.

Fig. 2 presents the experimental and fitted reflectance spectra by the DTL oscillator model with the dotted and solid lines, respectively. A good agreement is obtained in the entirely measured spectral region. It is worthy to mention that although the spectral profiles from six ceramics are similar, the reflectivity is different and varied with the La composition. Two evident peaks can be labeled as P_1 (~3.9 eV) and P_2 (~5 eV), whose variation with the La composition from the reflectivity are plotted in Figs. 2(b) and 2(c), respectively. The competition between the reflectance peak P_1 and P_2 can be observed and a surge of reflectance appears for the PLZST ceramics with the La composition of 2.6%. The derived dielectric functions ($\tilde{\varepsilon} = \varepsilon_1 + i\varepsilon_2$) of the PLZST ceramics are depicted in Fig. 3. Generally, with increasing the photon energy, the real part ε_1 increases and approaches the maximum at about 3.80 eV and then decreases due to the well-known Van Hover singularities. In the transparent region, the imaginary part ε_2 is close to zero and rapidly increases as the photon energy further increases, which indicates that the strong optical absorption appears. The dependence of the evaluated dielectric functions on the photon energy is very similar to those of the PZT and relative materials.[16] The main differences can be seen from the shoulders at about 4.8 eV and 4.3 eV in ε_1 and ε_2, respectively. It should be caused by the La introduction because the shoulder becomes more obvious as the La composition increases. In addition, the values of both ε_1 and ε_2 are varied with the La composition. The curves of the sample L1 and L2 almost overlap with a maximum point of 4.72 for ε_1. Whereas, the value over the calculated photon energy shifts drastically from sample L2.6 with the ε_1 maximum point of 6.92, then decreases steadily with the La composition. Note that the present dielectric constants derived from the near-infrared-ultraviolet region are much lower than the previous reported values, which are located in the infrared photon region.[17,18] It can be ascribed to the frequency dependence of optical functions.[11] As we know, there are some striking phonon mode contributions in the infrared range, especially for the complex perovskite-type structure.[19,20] Therefore, the infrared dielectric response should be enhanced, as compared to the interband electronic transitions. Nevertheless, the increment of the reflectivity and dielectric functions for the PLZST ceramic with the La composition of 2.6% appearing in the present work is abnormal, compared with the fact that the La substitution induced the monotone decreasing of the optical constants for relative materials reported in the infrared region.[17,18] The phenomena agree with the structural phase transition observed by the XRD pattern, which also undergoes at the La composition of 2.6%.

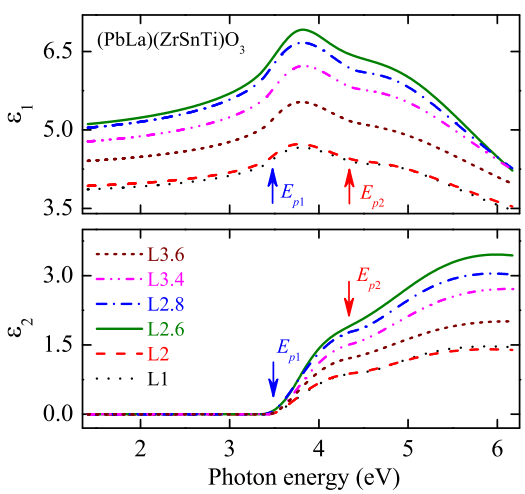

FIG. 3. The real and imaginary parts of the dielectric functions from the PLZST ceramics. The arrows indicate the positions of electronic band transitions.

Let us consider the DTL parameters in order to reveal the reason for the abnormal variation. A comparison of the DTL parameter values of the PLZST ceramics are listed in Table I. As previously discussed, the DTL model is determined by both Tauc joint density of states and the Lorentz oscillator.[15] The former is an empirical formula and the latter is obtained from standard quantum mechanical or Lorentz calculation. The fitting parameter E_p, from the Lorentz calculation, could be related to the *ab-initio* calculation. Three oscillators have been assigned to the corresponding transitions or excitations in several typical perovskite materials.[21,22] In similar ABO_3 perovskite material PZT, the valence-band maximum (VBM) is a mixture of O p and Pb s states at X with the $X_{4'v}$ symmetry, and the conduction-band minimum (CBM) is composed of the B ion d states as X_{3c} at low Zr composition and switches to A ion Pb $6p$-like states as X_{1c} while the Zr content increases.[23] In addition, there are nearly O p states as $X_{5'v}$ at the top of Γ (Γ_{15v}).[16] Lee *et al.* found three energy gaps E_a (~3.9 eV), E_b (~4.5 eV), and E_c (~6.5 eV) by fitting the second derivative of dielectric functions of PZT and relative materials. One can use the standard critical-point model to attribute three energy gaps to the transitions of $X_{4'v} \rightarrow X_{1c}$, $X_{5'v} \rightarrow X_{3c}$, and $X_{5'v} \rightarrow X_{1c}$, respectively.[16] Because E_c (~6.5 eV) is out of the experimental range, the present DTL parameters E_{p1} and E_{p2} can be uniquely corresponding to E_a and E_b of the PLZST material, respectively.

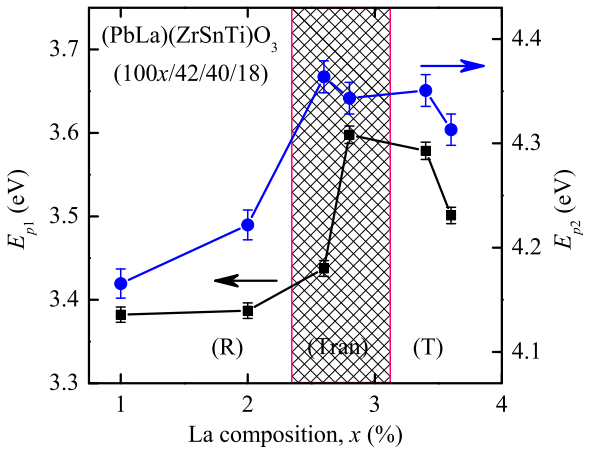

FIG. 4. Peak positions (E_{p1} and E_{p2}) of two oscillators as a function of the La composition for the PLZST ceramics. Note that the labels (R), (Tran), and (T) stand for the rhombohedral phase part, phase transition region, and tetragonal phase part, respectively. The error bars are directly taken from the experimental resolution.

Fig. 4 shows the E_p variation trend as a function of La composition. It could be distinctly divided into three parts: (i) the label "R" stands for rhombohedral phase part, (ii) the label "T" stands for tetragonal phase part, and (iii) between the two regions, the "Tran" is considered as a phase transition region. In the "R" region, both E_{p1} and E_{p2} change slightly with the phenomena of keeping the values of about 3.38 eV and 4.20 eV, respectively. In the "T" region, E_{p1} decreases from 3.59 eV to 3.50 eV and E_{p2} declines to 4.31 eV, which could be caused by the incorporation of La. By the first-principles density functional theory, Zhang *et al.*[24] suggested that the substitution of La for Pb introduces an impurity band in the forbidden band of PZT, leading to the reduction of the band gap. Note that this should be not evident at lower La composition. However, a blue shift could be observed in values of both E_{p1} and E_{p2} in the "Tran" region. As for the parameter E_{p1}, the value increases from 3.43 eV (L2.6) to 3.59 eV (L2.8). For the parameter E_{p2}, the value increases from 4.22 eV (L2) to 4.36 eV (L2.6). Compared the slight changes of energy gaps with the La composition in single-phased PZT and relative materials reported in the literatures,[16,23] the variations of energy gaps E_{p1} and E_{p2} at the La compositions of 2.6% and 2.8% are abnormally large. Moreover, the increment is contrary to the conclusion reported by Zhang *et al.*[24] Hence, it should be attributed to the changes of crystal structure during the process of phase transition.

As seen in Table I, the lattice parameters of the rhombohedral phase and tetragonal phase are different from each other. Furthermore, the ABO_3 peroskite structure is a three-dimensional network of regular corner-linked BO_6, octahedra with small B cations at the center of each octahedron and larger A cations being centrally located in the AO_{12} cuboctahedral cavity formed by eight octahedra. Substitution of La^{3+} for Pb^{2+} creates A-cation vacancies due to charge equilibrium and enhances the octahedral tilt angle owing to smaller ironic radius.[25] The octahedral tilting is the most commonly occurring distortion and is also a major contributor to the structural variability.[26] Through high-pressure neutron powder diffraction experiments and density functional theory computation on lead titanate ($PbTiO_3$), a competition is demonstrated between oxygen octahedral tilting and entropy. The octahedral tilting gives advantage for the rhombohedral phase and the entropy favors the tetragonal phase above 130 K. The octahedral tilting often occurs as it allows energy minimization by changing the bond lengths and angles.[27] A complex mechanism caused by the variation of bond lengths and angles in crystal lattice could substantially contribute to the changes of electronic band structure. Therefore, it can result in an anomalous variation of the optical properties, such as reflectance and dielectric functions.

In summary, La modified lead zironate titanate ceramics (PLZST, 100x/42/40/18) with different composition ($x = 1\%$, 2%, 2.6%, 2.8%, 3.4%, and 3.6%) have been investigated near morphotropic phase boundary. A significant difference in the XRD patterns is observed between $x = 2.6\%$ and $x = 2.8\%$, which is attributed to the phase transition from the rhombohedral to tetragonal structure. A relatively high dielectric function is obtained when the phase transition occurs. The critical points related model parameters, E_{p1} and E_{p2}, show a blue shift trend, indicating abnormal variation of the electronic structure near the MPB region.

This work was financially supported by Major State Basic Research Development Program of China (Grant No. 2011CB922200), Natural Science Foundation of China (Grant Nos. 11074076 and 60906046), Projects of Science and Technology Commission of Shanghai Municipality (Grant Nos. 11520701300, 10DJ1400201, and 10SG28), and the Program for Professor of Special Appointment (Eastern Scholar) at Shanghai Institutions of Higher Learning.

[1]A. S. Mischenko, Q. Zhang, J. F. Scott, R. W. Whatmore, and N. D. Mathur, Science **311**, 1270 (2006).
[2]J. Y. Li, R. C. Rogan, E. Üstündag, and K. Bhattacharya, Nature Mater. **4**, 776 (2005).
[3]G. H. Haertling, J. Am. Cream. Soc. **82**, 797 (1999).
[4]D. S. L. Pontes, L. Gracia, F. M. Pontes, A. Beltrán, J. Andrés, and E. Longo, J. Mater. Chem. **22**, 6587 (2012).
[5]N. Luo, Y. Li, Z. Xia, and Q. Li, CrystEngComm **14**, 4547 (2012).
[6]D. Berlincourt, IEEE Trans. Sonics Ultrason. **13**, 116 (1966).
[7]H. L. Zhang, X. F. Chen, F. Cao, G. S. Wang, X. L. Dong, Y. Gu, and Y. S. Liu, Appl. Phys. Lett. **94**, 252902 (2009).
[8]H. L. Zhang, X. F. Chen, F. Cao, G. S. Wang, X. L. Dong, Y. Gu, H. L. He, and Y. S. Liu, J. Appl. Phys. **108**, 086105 (2010).
[9]E. Breval, C. Wang, and J. P. Dougherty, J. Am. Ceram. Soc. **88**, 437 (2005).
[10]W. Chan, Z. Xu, T. F. Hung, and H. Chen, J. Appl. Phys. **96**, 6606 (2004).
[11]A. B. Djurišić, Y. Chan, and E. H. Li, Mater. Sci. Eng. R **38**, 237 (2002).
[12]Y. Li, L. Qiang, L. Wang, Z. Yang, and X. Chu, J. Cryst. Growth **318**, 860 (2011).
[13]L. Xue, Q. Li, Y. Zhang, X. Zhen, R. Liu, and L. Wang, J. Cryst. Growth **283**, 378 (2005).
[14]E. Breval, C. Wang, and J. P. Dougherty, J. Am. Ceram. Soc. **88**, 437 (2005).
[15]J. G. E. Jellison and F. A. Modine, Appl. Phys. Lett. **69**, 371 (1996); **69**, 2137 (1996)
[16]H. Lee, Y. S. Kang, S. Cho, B. Xiao, H. Morkoç, T. D. Kang, G. S. Lee, J. Li, S. Wei, P. G. Snyder, and J. T. Evans, J. Appl. Phys. **98**, 094108 (2005).
[17]Z. G. Hu, F. W. Shi, T. Lin, Z. M. Huang, G. S. Wang, Y. N. Wu, and J. H. Chu, Phys. Lett. A **320**, 478 (2004).
[18]Z. G. Hu, F. W. Shi, Z. M. Huang, Y. N. Wu, G. S. Wang, and J. H. Chu, Appl. Phys. A **80**, 841 (2003).
[19]E. Buixaderas, D. Nuzhnyy, J. Petzelt, L. Jin, and D. Damjanovic, Phys. Rev. B **84**, 184302 (2011).
[20]K. Jiang, J. Z. Zhang, W. L. Yu, Z. G. Hu, and J. H. Chu, Appl. Phys. A **106**, 877 (2012).

[21]W. W. Li, J. J. Zhu, J. D. Wu, J. Gan, Z. G. Hu, M. Zhu, and J. H. Chu, Appl. Phys. Lett. **97**, 121102 (2010).
[22]P. Chen, N. J. Podraza, X. S. Xu, A. Melville, E. Vlahos, V. Gopalan, R. Ramesh, D. G. Schlom, and J. L. Musfeldt, Appl. Phys. Lett. **96**, 131907 (2010).
[23]W. L. Warren, J. Robertson, D. Dimos, B. A. Tuttle, G. E. Pike, and D. A. Payne, Phys. Rev. B **53**, 3080 (1996).
[24]Z. Zhang, P. Wu, K. Ong, L. Lu, and C. Shu, Phys. Rev. B **76**, 125102 (2007).
[25]R. S. Solanki, A. K. Singh, S. Mishra, S. Kennedy, T. Suzuki, Y. Kuroiwa, C. Moriyoshi, and D. Pandey, Phys. Rev. B **84**, 144116 (2011).
[26]C. J. Howard and H. T. Stokes, Acta Crystallogr., Sect. A: Cryst. Phys., Diffr., Theor. Gen. Crystallogr. **61**, 93 (2005).
[27]J. Frantti, Y. Fujioka, J. Zhang, S. C. Vogel, Y. Wang, Y. Zhao, and R. M. Nieminen, J. Phys. Chem. B **113**, 7967 (2009).